Frequency dependence of the admittance of a quantum point contact

I. E. Aronov
Sage Technology Inc., 1800 Sandy Plains Parkway, Suite 320, Marietta, Georgia 30066

N. N. Beletskii
Institute of Radiophysics and Electronics, National Academy of Sciences of Ukraine, 12 Acadamia Proskura Street, 310085, Kharkov, Ukraine

G. P. Berman
Theoretical Division and CNLS, Los Alamos National Laboratory, Los Alamos, New Mexico 87545

D. K. Campbell
Department of Physics, University of Illinois at Urbana-Champaign, 1110 West Green Street, Urbana, Illinois 61801-3080

G. D. Doolen
Theoretical Division and CNLS, Los Alamos National Laboratory, Los Alamos, New Mexico 87545

S. V. Dudiy
Institute of Radiophysics and Electronics, National Academy of Sciences of Ukraine, 12 Acadamia Proskura Street, 310085, Kharkov, Ukraine

(Received 9 March 1998)

Using a Boltzmann-like kinetic equation derived in the semiclassical approximation for the partial Wigner distribution function, we determine the ac admittance of a two-dimensional quantum point contact (QPC) for applied ac fields in the frequency range $\omega \approx 0-50$ GHz. We solve self-consistently an integral equation for the spatial distribution of the potential inside the QPC, taking into account the turning points of the semiclassical trajectories. The admittance of the QPC is a strong function of the gate voltage. This gate voltage can be used to ''tune'' the number of open channels (N) for electron transport. We show that, for most values of gate voltage, the imaginary part of the total admittance is positive for $N>1$, so that the QPC has an inductive character, because of the predominant role of the open channels. In contrast, for $N=0$ or 1, for most values of the gate voltage, the imaginary part of the admittance is negative, corresponding to capacitive behavior. For gate voltages near values at which channels open or close, very strong nonlinear effects arise, and the admittance oscillates rapidly (with its imaginary part sometimes changing sign) both as the function of gate voltage (at fixed frequency) and as a function of frequency (at fixed gate voltage). Experimental observation of these oscillations would provide an important test of our semiclassical approach to the ac response of a QPC. We explore the low-frequency regime and investigate the extent to which one can understand the admittance in terms of a static conductance and a ''quantum capacitance'' and a ''quantum inductance.'' We show that it is possible to choose the gate voltage so that there is a large, low-frequency regime in which the admittance is well approximated by a linear function of frequency. In this regime, the admittance can be treated by ''equivalent circuit'' concepts. We study how this approach breaks down at higher frequencies, where strongly nonlinear behavior of the admittance arises. We estimate the value of frequency, ω_c, at which the crossover from the low-frequency linear regime to the high-frequency nonlinear behavior occurs. For chosen parameters of a QPC, $\omega_c \approx 10$ GHz. [S0163-1829(98)02339-X]

I. INTRODUCTION

The quantum point contact (QPC) is one of the fundamental nanocircuit elements. QPC's are typically made by putting a split gate on the top of a GaAs-$Al_xGa_{1-x}As$ heterostructure and applying a voltage to the gate to create a constriction of variable width in a two-dimensional electron gas (2DEG) (see Fig. 1). QPC's display many unusual behaviors, including steplike oscillations of the conductance as a function of the gate voltage. The intense interest in these QPC's is reflected in the large literature, both experimental and theoretical, that has arisen in the decade since their introduction (see, for example, Refs. 1–22).

Recently, it was shown[1–5] that a QPC displays interesting quantum effects not only in dc transport but also in response to an ac field, where it exhibits quantum inductive[20] and capacitive[17,20] behavior (see also Ref. 23, where quantum inductance was introduced for mesoscopic systems and applied to a resonant tunneling device). This suggests that a QPC can be considered as an elementary circuit of extremely small size, $\sim 0.1-1$ μm.

In a previous paper,[20] we developed an approach, based on a variant of the Wigner distribution function (WDF) formalism, for calculating the ac transport through a QPC. Using this method, we were able to demonstrate[20] that *in the low-frequency regime* the admittance of the QPC can indeed

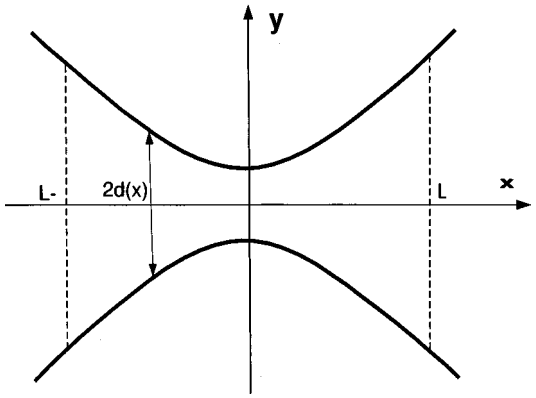

FIG. 1. The geometry of the constriction. The width is denoted by $2d(x)$, the narrowest width is $2d(0)$, and the effective length is $2L$.

be calculated using a simple equivalent circuit that includes resistive, capacitive, and inductive components. In particular, in the low-frequency regime, the QPC's admittance consists of a conductance (the real part of the admittance) and an *emittance*[17] that includes inductive and capacitive effects, which we shall henceforth call quantum capacitance[17] and quantum inductance.[20] The emittance is sensitive to the geometry of the QPC and can be controlled by the gate voltage. We also showed[20] that stepwise jumps in the quantum inductance are determined by the harmonic mean of the velocities of the propagating modes (open channels) through the QPC, whereas the quantum capacitance is a mesoscopic manifestation of the reflected electron modes.

Importantly, as introduced, the concepts of quantum *inductance* and quantum *capacitance* apply for the QPC *only* in the regime of low frequency and for values of the gate voltage far from the voltages where the electron modes appear or disappear (''opening points''). In the high-frequency regime, and near the gate voltages at which new electron modes appear (or disappear), the frequency dispersion of the admittance becomes nonlinear and complicated. In this case, the QPC cannot be described (at least not using a simple circuit as in Ref. 20) by static (i.e., frequency-independent) conductance, inductance, and capacitance. Consequently, to understand the QPC response to an ac field, it is necessary to investigate the frequency dependence of the admittance as a distributed mesoscopic characteristic of the QPC.

In this paper, we investigate the frequency dependence of the admittance for the symmetric QPC in the form of a smooth constriction (adiabatic geometry) without making a low-frequency approximation. In Sec. II, we derive the integral equation for the spatial distribution of the electric potential inside the QPC and use it to determine an explicit expression for the admittance. In Sec. III, we study numerically the integral equation for the potential for frequencies in the range $\omega \approx 0-50$ GHz, as a function of the width of the QPC and the number of open and closed channels. We find that there is a characteristic value of frequency ω_c at which the system crosses over from a linear dependence on frequency characterized by static conductance, capacitance, and inductance to a strongly nonlinear dependence on frequency. For chosen values of QPC parameters, $\omega_c \sim 10$ GHz. In the frequency region $\omega > \omega_c \sim 10$ GHz, the admittance of the QPC displays several characteristic nonlinear features. In the neighborhood of channel openings, the admittance exhibits oscillations as a function of the parameter $q = 2k_F d(0)/\pi$ [where k_F is a Fermi wave vector and $2d(0)$ is the minimum width of the QPC]. In our approach, these oscillations arise from the behavior of trajectories close to the ''separatrix'' of the semiclassical motion. Experimental confirmation (or refutation) of the existence of these oscillations would provide an important test of our approach to the ac transport in the QPC. In Sec. IV, we summarize our results.

II. SPATIAL DISTRIBUTION OF THE POTENTIAL IN THE QPC AND THE ADMITTANCE

We have previously shown[20] how to use the partial Wigner distribution function (PWDF) formalism, to find the charge, $\rho_n(x)$, and the current, $j_n(x)$, densities in the QPC. For open channels, we have

$$\rho_n(x) = \frac{2e^2}{h}\frac{1}{v_n(x)}\int_{-L}^{L} dx' E(x')\,\mathrm{sgn}(x-x') \times \exp[i\omega^* \tau_n(x,x')\,\mathrm{sgn}(x-x')], \tag{1}$$

and

$$j_n(x) = \frac{2e^2}{h}\int_{-L}^{L} dx' E(x')\exp[i\omega^* \tau_n(x,x')\,\mathrm{sgn}(x-x')]. \tag{2}$$

In Eq. (2), $E(x)$ is the spatial envelope of the electric field inside the QPC: $E(x,t) = -[\partial\Phi(x)/\partial x]\exp(-i\omega t)$; $2L$ is the length of the constriction shown in Fig. 1; $\omega^* = \omega + i\nu$, with $1/\nu$ being the momentum relaxation time,

$$\tau_n(x,x') = \int_{x'}^{x} \frac{dx''}{v_n(x'')}; \tag{3}$$

and $v_n(x)$ is the velocity of an electron in the nth channel. For the closed channels (reflecting modes) we have

$$\rho_n(x) = \frac{2e^2}{h}\frac{\mathrm{sgn}(x)}{v_n(x)}\int_{x_n}^{L} dx' E(x'\ \mathrm{sgn}(x)) \times \{\mathrm{sgn}(|x|-x')\exp[i\omega^* \tau_n(|x|,x')\,\mathrm{sgn}(|x|-x')] - \exp[i\omega^*(\tau_n(|x|,x_n)+\tau_n(x',x_n))]\}\,\theta(|x|-x_n), \tag{4}$$

$$j_n(x) = \frac{2e^2}{h}\int_{x_n}^{L} dx' E(x'\ \mathrm{sgn}(x)) \times \{\exp[i\omega^* \tau_n(|x|,x')\,\mathrm{sgn}(|x|-x')] - \exp[i\omega^*(\tau_n(|x|,x_n)+\tau_n(x',x_n))]\}\,\theta(|x|-x_n). \tag{5}$$

Here x_n is the absolute value of the critical (turning) point, which is determined by the condition,

$$\varepsilon_n(x_n)=\mu. \tag{6}$$

The velocities v_n are defined by

$$v_n=\sqrt{(2/m)(\mu-\varepsilon_n(x))}. \tag{7}$$

In Eqs. (6) and (7), m is the effective mass of the electron, μ is the chemical potential, and

$$\varepsilon_n(x)=\frac{\pi^2 n^2\hbar^2}{8md^2(x)} \tag{8}$$

is a transverse electron energy in the QPC, with $2d(x)$ being the width of the (assumed adiabatic) constriction (see Fig. 1). Here, as in Ref. 20, we focus on ballistic transport only. This means that we assume that the effects of disorder and dissipation on the transport characteristics of the QPC are not significant and can be neglected to leading order as $\nu\to 0$. For sufficiently high frequencies of the electric field, small corrections to the transport characteristics caused by weak disorder and dissipation effects are taken into account in Eqs. (1)–(5) by having $\nu\neq 0$. We assume that the relaxation frequency ν satisfies $\nu\ll v_F/L$ and $\nu\ll\omega$, where v_F is the Fermi velocity.

One can see from Eqs. (1)–(5) that the transport through a QPC is described by highly nonlocal (integral) operators. This (correctly) suggests that the charge and current densities at a given point x are influenced by the electric field generated throughout the whole constriction. Thus, the PWDF formalism allows us to derive the charge and the current densities as nonlocal functions of the electric field.

In Eqs. (1) and (2) the electric field can be calculated using the Poisson equation for the two-dimensional (2D) electron layer,[24]

$$\Delta\Phi(x,y,z)=-\frac{4\pi}{\epsilon}\,\rho(x,y)\,\delta(z), \tag{9}$$

where $\rho(x,y)$ is the charge density,

$$\rho(x,y)=\sum_n \rho_n(x)\Psi_n^2(y), \tag{10}$$

and ϵ is the dielectric constant. For simplicity, we do not indicate explicitly dependence on time in Eqs. (9) and (10). In Ref. 9, $\Phi(x,y,z)$ is the electric potential; $\Psi_n(y)$ is the transverse wave function of an electron in the adiabatic QPC, satisfying $\Psi_n(\pm d(x))=0$.[20]

The Fourier transform and the inverse transform in the x direction are

$$\Phi(k_x,y,z)=\int_{-\infty}^{\infty}dx\Phi(x,y,z)\exp(-ik_x x),$$
$$\Phi(x,y,z)=\frac{1}{2\pi}\int_{-\infty}^{\infty}dk_x\Phi(k_x,y,z)\exp(ik_x x). \tag{11}$$

The δ function in Eq. (9) allows[24] the Fourier transform of the electric potential, $\Phi(x,y,z)$, in the QPC to be represented as

$$\Phi(k_x,k_y,z)=\Phi(k_x,k_y,z=0)\exp(-k|z|), \tag{12}$$

where $k=\sqrt{k_x^2+k_y^2}$. The expression for $\Phi(k_x,y)\equiv\Phi(k_x,y,z=0)$ is

$$\Phi(k_x,y)=(1/\epsilon)\int_{-d(x)}^{d(x)}dy'\times\int_{-\infty}^{\infty}dk_y\,\frac{\exp[ik_y(y-y')]}{\sqrt{k_x^2+k_y^2}}\,\rho(k_x,y'). \tag{13a}$$

From Eq. (13a), we see that $\Phi(k_x,y)$ also depends (weakly, given our assumption of adiabaticity) on x through the integration limits, $\pm d(x)$. For $|y|\gg d$ and $|y|\ll 1/k_x$, the potential $\Phi(k_x,y)$ decreases exponentially with $|y|$: $\Phi(k_x,y)\sim\exp(-|k_x y|)$. Indeed, if we integrate over k_y in Eq. (13a),

$$\Phi(k_x,y)=(2/\epsilon)\int_{-d(x)}^{d(x)}K_0(|k_x(y-y')|)\rho(k_x,y')dy', \tag{13b}$$

and set $|y-y'|\simeq|y|(|y'|\leqslant d,|y|\gg d)$ we find

$$\Phi(k_x,y)\simeq(2/\epsilon)K_0(|k_x y|)\int_{-d(x)}^{d(x)}\rho(k_x,y')dy'. \tag{13c}$$

One can see from Eq. (13c) that outside the constriction the dependence of the potential $\Phi(k_x,y)$ on the transverse coordinate y is determined by the MacDonald function, $K_0(|k_x y|)$.[25] Replacing $K_0(|k_x y|)$ by its asymptotic form for $|k_x y|\gg 1$, we obtain

$$\Phi(k_x,y)\simeq\epsilon^{-1}\sqrt{2\pi/|k_x y|}\exp(-|k_x y|)\times\int_{-d(x)}^{d(x)}\rho(k_x,y')dy'. \tag{13d}$$

For our further calculations, we need the value of $\Phi(x,y)$ averaged over the transverse coordinate, y. From Eq. (13a) we find

$$\overline{\Phi}(k_x)\equiv\frac{1}{2d(x)}\int_{-d(x)}^{d(x)}dy\Phi(k_x,y). \tag{14}$$

We define

$$\rho_n(k_x)=\int_{-\infty}^{\infty}dx\rho_n(x)\exp(-ik_x x). \tag{15}$$

We shall use the following boundary conditions for the Poisson Eq. (9):

$$\Phi(-L)=V/2,\quad \Phi(L)=-V/2. \tag{16}$$

The expression for $\Phi(x)$ is

$$\Phi(x)\equiv\frac{1}{2\pi}\int_{-\infty}^{\infty}dk_x\overline{\Phi}(k_x)\exp(ik_x x)=\frac{1}{2\pi\epsilon}\sum_n\int_{-\infty}^{\infty}dx'\rho_n(x')Q_n(x,x'), \tag{17}$$

where

$$Q_n(x,x')=\frac{(2\pi n)^2}{d(x)}\int_0^\infty d\xi\,\frac{\sin^2\xi}{\xi^2[(\pi n)^2-\xi^2]}\,K_0\left[\frac{|x-x'|}{d(x)}\,\xi\right]. \tag{18}$$

In Eq. (18), $K_0[z]$ is again the MacDonald function. Recall that we have assumed that the electric field inside the QPC has the form $E(x,t)=-[\partial\Phi(x)/\partial x]\exp(-i\omega t)$.

The admittance is determined from

$$Y=\frac{I_{\rm tot}}{V}=\frac{1}{V}\sum_n j_n(-L)$$

$$=\frac{1}{V}\sum_{n=1}^{N} j_n^{(o)}(-L)+\frac{1}{V}\sum_{n=N+1}^{N+\tilde{N}} j_n^{(c)}(-L), \tag{19}$$

where $I_{\rm tot}$ is the total current through the QPC, and

$$N=\left[\frac{2k_Fd(0)}{\pi}\right],\quad \tilde{N}=\left[\frac{2k_Fd(0)}{\pi}\exp(L/\tilde{L})^2\right]-N,$$

$$d(x)=d(0)\exp[(x/\tilde{L})^2]. \tag{20}$$

In Eq. (20), $\hbar k_F=\sqrt{2m\mu}$, $[z]$ is the integer part of z, N is the number of open channels, $\tilde{N}$ is the number of closed channels, and $\tilde{L}$ is a parameter that characterizes the smoothness of the QPC.

From Eq. (19) we see clearly that one must know the *spatial distribution* of the electric field inside the QPC in order to calculate the admittance. To solve this problem, we introduce the following dimensionless parameters and variables:

$$\Phi(x)=V\phi(\zeta),\quad x=L\zeta,\quad x'=L\zeta',\quad x_n=L\zeta_n,$$

$$\alpha=\frac{e^2}{hv_F},\quad \beta=\beta'+i\beta''=\frac{\omega^*L}{v_F},\quad q=\frac{2k_Fd(0)}{\pi},$$

$$N=[q],\quad \tilde{N}=[q\,\exp(L/\tilde{L})^2]-N, \tag{21}$$

$$f_n(\zeta)\equiv\frac{v_n(\zeta)}{v_F}=\left\{1-\frac{n^2}{q^2}\exp\left[-2\left(\frac{L}{\tilde{L}}\right)^2\zeta^2\right]\right\}^{1/2}, \tag{22}$$

and the dimensionless functions

$$Q_n(\zeta,\zeta')=\frac{L}{d(\zeta)}\,(2\pi n)^2\int_0^\infty dt\,\frac{\sin^2 t}{t^2[(\pi n)^2-t^2]}\times K_0\left[t|\zeta-\zeta'|\,\frac{L}{d(\zeta)}\right],$$

$$d(\zeta)=d(0)\exp\left[\left(\frac{L}{\tilde{L}}\right)^2\zeta^2\right],$$

$$\psi_n(\zeta)=\tfrac{1}{2}\{\exp[i\beta\tau_n(\zeta,-1)]-\exp[-i\beta\tau_n(\zeta,1)]\},$$

$$\tilde{\psi}_n(\zeta)=-\tfrac{1}{2}\,\mathrm{sign}(\zeta)\{\exp[-i\beta\tau_n(|\zeta|,1)]+\exp[i\beta(\tau_n(|\zeta|,\zeta_n)+\tau_n(1,\zeta_n))]\},$$

$$\tau_n(\zeta_1,\zeta_2)\equiv\int_{\zeta_2}^{\zeta_1}\frac{d\zeta}{f_n(\zeta)},$$

$$P_n(\zeta,\zeta')\equiv\exp[i\beta\,\mathrm{sign}(\zeta-\zeta')\tau_n(\zeta,\zeta')],$$

$$q_n(\zeta,\zeta')=\exp[i\beta\tau_n(|\zeta|,\zeta')\mathrm{sign}(|\zeta|-\zeta')]+\exp\{i\beta[\tau_n(|\zeta|,\zeta_n)+\tau_n(\zeta',\zeta_n)]\}.$$

The integral equation for the electric potential $\phi(\zeta)$ follows from Eqs. (1) and (17) and has the form

$$\phi(\zeta)=\frac{\alpha}{\pi\epsilon}\{F(\zeta)+\hat{F}_1[\phi(\zeta)]-i\beta\hat{F}_2[\phi(\zeta)]\}. \tag{23}$$

In Eq. (23),

$$F(\zeta)=\sum_{n=1}^{N}\int_{-1}^{1}d\zeta'Q_n(\zeta,\zeta')\,\frac{\psi_n(\zeta')}{f_n(\zeta')}+\sum_{n=N+1}^{N+\tilde{N}}\int_{-1}^{1}d\zeta'Q_n(\zeta,\zeta')\,\frac{\tilde{\psi}_n(\zeta')}{f_n(\zeta')}\,\Theta(|\zeta'|-\zeta_n), \tag{24}$$

$$\hat{F}_1[\phi(\zeta)]=-2\sum_{n=1}^{N}\int_{-1}^{1}d\zeta'Q_n(\zeta,\zeta')\,\frac{\phi(\zeta')}{f_n(\zeta')}-2\sum_{n=N+1}^{N+\tilde{N}}\int_{-1}^{1}d\zeta'Q_n(\zeta,\zeta')\Theta(|\zeta'|-\zeta_n)\times\frac{\phi(\zeta')}{f_n(\zeta')}, \tag{25}$$

$$\hat{F}_2[\phi(\zeta)]=\sum_{n=1}^{N}\int_{-1}^{1}d\zeta'Q_n(\zeta,\zeta')\,\frac{1}{f_n(\zeta')}\times\int_{-1}^{1}d\zeta_2\phi(\zeta_2)\,\frac{P_n(\zeta',\zeta_2)}{f_n(\zeta_2)}+\sum_{n=N+1}^{N+\tilde{N}}\int_{-1}^{1}d\zeta'Q_n(\zeta,\zeta')\,\frac{\Theta(|\zeta'|-\zeta_n)}{f_n(\zeta')}\times\int_{\zeta_n}^{1}d\zeta_2\phi[\zeta_2\,\mathrm{sign}(\zeta')]\,\frac{q_n(\zeta',\zeta_2)}{f_n(\zeta_2)}. \tag{26}$$

Assuming that the electric potential $\phi(\zeta)$ is the solution of Eqs. (23)–(26), we can represent the admittance in Eq. (19) in the form

$$Y=\frac{2e^2}{h}\,y, \tag{27}$$

where the dimensionless admittance y is given by the following expression, which depends functionally on $\phi(\zeta)$:

$$y=\sum_{n=1}^{N}y_n^{(o)}+\sum_{n=N+1}^{N+\tilde{N}}y_n^{(c)}. \tag{28}$$

In Eq. (28), $y_n^{(o)}$ is the contribution to the admittance from the open channels and $y_n^{(c)}$ is the contribution to the admittance from the closed channels, and their functional dependence on $\phi(\zeta)$ is given by

$$y_n^{(o)} = \tfrac{1}{2}\{\exp[i\beta\tau_n(1,-1)]+1\} + i\beta \times \int_{-1}^{1} d\xi\phi(\zeta)\,\frac{\exp[i\beta\tau_n(\zeta,-1)]}{f_n(\zeta)}, \tag{29}$$

$$y_n^{(c)} = \tfrac{1}{2}\{1-\exp[2i\beta\tau_n(1,\zeta_n)]\} - i\beta\int_{\zeta_n}^{1} d\zeta\,\frac{\phi(\zeta)}{f_n(\zeta)}\{\exp[i\beta\tau_n(1,\zeta)] + \exp[i\beta\tau_n(1,\zeta_n)+\tau_n(\zeta,\zeta_n)]\}. \tag{30}$$

III. RESULTS OF NUMERICAL SIMULATIONS

We solved the integral equation (23) for the potential, $\phi(\zeta)=\phi'(\zeta)+i\phi''(\zeta)$ and numerically evaluated the expressions (28)–(30) for the admittance, $y=y'+iy''$. Here and henceforth, we follow the convention that a superscript $'$ indicates the real part, and superscript $''$ indicates the imaginary part, of the corresponding quantity. For the parameters of the QPC, we used values that correspond to the $Ga_xAl_{1-x}As/GaAs$ heterostructure studied experimentally by Mailly, Chapelier, and Benoit:[26]

$$\epsilon=13, \quad v_F=2.6\times10^7 \text{ cm/s}, \quad k_F=1.5\times10^6 \text{ cm}^{-1}, \quad d(0)\sim10^{-6} \text{ cm}, \quad L\sim10^{-3} \text{ cm}. \tag{31}$$

The integral equation (23) is a Fredholm equation of the second kind, and we solved it using the Nystrom method with the Gauss-Legendre quadrature.[27,28] For calculating $F(\zeta)$ and the kernels of the integral operators $\hat{F}_1, \hat{F}_2$ in Eq. (23), it is necessary to consider that the integrals in Eqs. (24)–(26) contain integrable singularities. As $\zeta-\zeta'\to0$, $Q_n(\zeta,\zeta')$ is proportional to $\ln|\zeta-\zeta'|$. Moreover, for the closed channels ($N+\tilde{N}\geqslant n\geqslant N+1$), when $|\zeta|$ approaches the turning point ζ_n we have

$$1/f_n(\zeta)\sim\theta(|\zeta|-\zeta_n)/\sqrt{\zeta_n(|\zeta|-\zeta_n)}. \tag{32}$$

In the neighborhood of the singularities, we replace the functions $Q_n(\zeta,\zeta')$ and $1/f_n(\zeta)$ in the integrand by the appropriate asymptotic expressions. In the integrals in Eqs. (24)–(26), for ζ near one of the turning points, $\pm\zeta_n$, ($n=N+1,\ldots,N+\tilde{N}$), the square root singularity in $1/f_n(\zeta)$ and the logarithmic singularity in $Q_n(\zeta,\zeta')$ reinforce each other, and hence the potential, $\phi(\zeta)$, has a peak type at the turning points (see Figs. 2 and 3). The potential curves 1–5 in Fig. 2 correspond to the different values of the frequency ω [or the dimensionless frequency, β' in Eq. (21)]. The potential curves 1–3 in Fig. 3 correspond to the different values of the relaxation frequency ν (or the dimensionless parameter β'').

As one can see from Figs. 2(a) and 3(a), the values of the real part of the potential at the boundary of the QPC [$\phi'(\pm1)$] are slightly different from the values required by the boundary conditions (16), $\phi(\mp1)=\pm1/2$. The reason for this is that in deriving the integral Eq. (23) for the potential, we assumed that the boundary conditions (16) are actually the equations for the edges ($x=\pm L$, or for the dimensionless parameter, $L/\tilde{L}$) of the constriction shown in Fig. 1. To explore the effects of the boundary conditions more carefully, we calculated numerically the value of the parameter $L/\tilde{L}$ for which the boundary conditions *were* satisfied. Compared with the numerical results for $\phi'(\zeta)$ shown in Figs. 2(a) and 3, which were obtained for $\tilde{L}=L$ or $L/\tilde{L}=1$, we found [see Figs. 4(a) and 4(b)] that for $L/\tilde{L}=1.4$ the required boundary conditions, $\phi(\mp1)=\pm1/2$, were more accurately satisfied. Importantly, our numerical results show that the details of the behavior of the potential in the vicinity of the edges ($x=\pm L$) of the QPC shown in Fig. 1 influence only weakly the behavior of the admittance, y, in Eq. (28). This is demonstrated in Figs. 5(a) and 5(b), where the curves 1–3 in each of these figures correspond to different values of the parameter $L/\tilde{L}$. As usual, the indices (o) and (c) indicate the contribution to the admittance from open and closed channels, respectively.

Our numerical simulations show that if the value of q

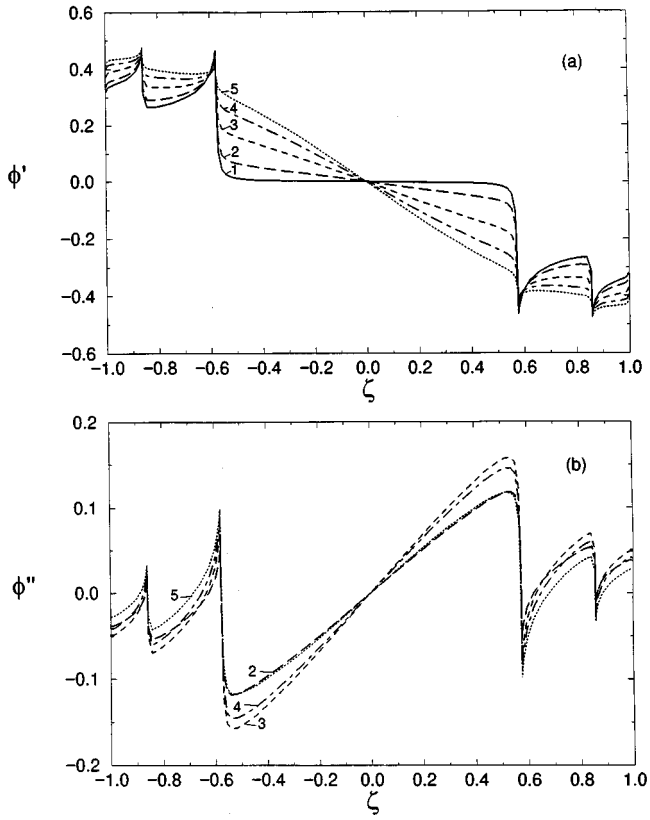

FIG. 2. Spatial distribution of the potential $\phi(\zeta)$ ($\zeta=x/L$) in the QPC for different values of frequency ω. (a) The real part of the potential $\phi'(\zeta)$; (b) the imaginary part, $\phi''(\zeta)$. Curves 1–5 correspond to $\beta'=0$ ($\omega=0$), $\beta'=0.5$ ($\omega=1.3\times10^{10}$ s^{-1}), $\beta'=1.0$ ($\omega=2.6\times10^{10}$ s^{-1}), $\beta'=1.5$ ($\omega=3.9\times10^{10}$ s^{-1}), and $\beta'=2.0$ ($\omega=5.2\times10^{10}$ s^{-1}), respectively. In Fig. 2(b), curve 1 is not shown because in the static case $\phi''(\zeta)\equiv0$. The parameters of the QPC are $d(0)=1.5\times10^{-6}$ cm, $L=\tilde{L}=10^{-3}$ cm (so $q=2k_Fd(0)/\pi=1.43$, $N=1$, $\tilde{N}=2$), and $\nu=0$. The value of q is not close to an integer. The potential is a stepwise function of the longitudinal coordinate ζ, with the steps having peaks at the turning points.

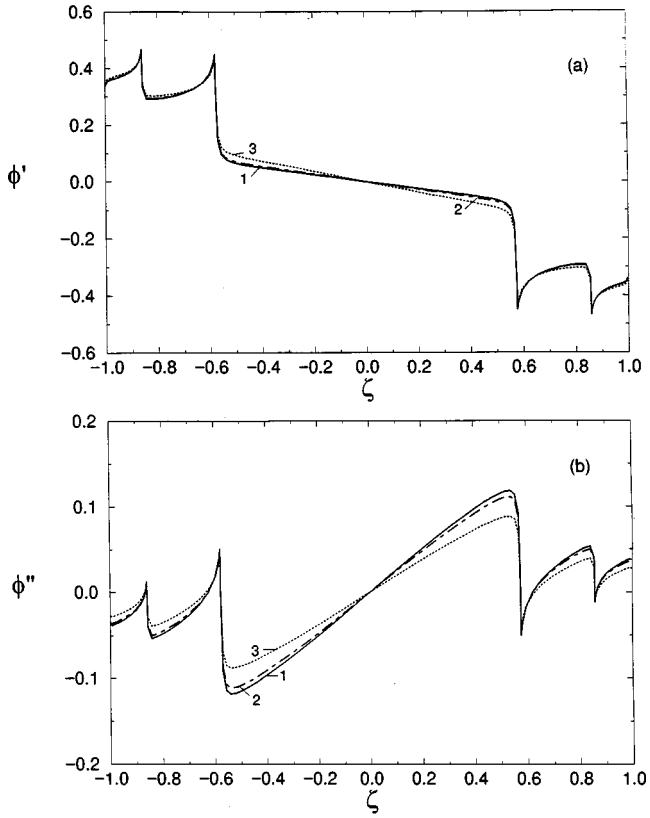

FIG. 3. Dependence of the potential profile $\phi(\zeta)$ on the relaxation frequency ν (or $\beta''=\nu L/v_F$). (a) The real part of ϕ; (b) the imaginary part of ϕ. The curves are presented for $\nu=0, \beta''=0$ (curve 1); $\nu=1.0\times10^9\ \mathrm{s}^{-1}$, $\beta''=0.038$ (curve 2); $\nu=5.0\times10^9\ \mathrm{s}^{-1}$, $\beta''=0.19$ (curve 3) at $\beta'=0.5$ ($\omega=1.3\times10^{10}\ \mathrm{s}^{-1}$). As in Fig. 2, the values of the parameters are $d(0)=1.5\times10^{-6}$ cm, $L=\tilde{L}=10^{-3}$ cm [so $q=2k_Fd(0)/\pi=1.43, N=1, \tilde{N}=2$], and $\nu=0$.

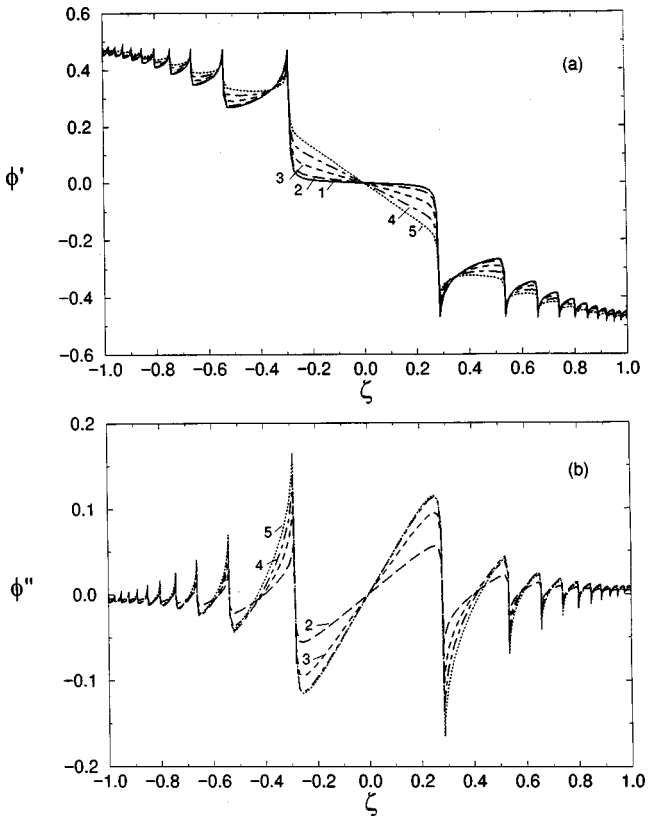

FIG. 4. Spatial distribution of the potential $\phi(\zeta)$ ($\zeta=x/L$) in the QPC for different values of frequency ω when $L/\tilde{L}=1.4, \tilde{L}=10^{-3}$ cm, $q=1.7$ [$d(0)=1.5\times10^{-6}$ cm, $N=1, \tilde{N}=11$] and $\nu=0$. (a) The real part of the potential $\phi'(\zeta)$; (b) the imaginary part, $\phi''(\zeta)$. Curves 1–5 correspond to $\beta'=0$ ($\omega=0$), $\beta'=0.5$ ($\omega=0.9\times10^{10}\ \mathrm{s}^{-1}$), $\beta'=1.0$ ($\omega=1.9\times10^{10}\ \mathrm{s}^{-1}$), $\beta'=1.5$ ($\omega=2.8\times10^{10}\ \mathrm{s}^{-1}$), and $\beta'=2.0$ ($\omega=3.7\times10^{10}\ \mathrm{s}^{-1}$) In Fig. 4(b), curve 1 is not shown because in the static case $\phi''(\zeta)\equiv0$.

$=2k_Fd(0)/\pi$ is not close to an integer, the potential profile has the characteristic form shown in Figs. 2 and 3. In the spatial region between the first turning points $-\zeta_{N+1}$ and ζ_{N+1} (the closest turning points to the center of the QPC, $\zeta=0$), the real part of the potential, $\phi'(\zeta)$, is a monotonic function of the longitudinal coordinate ζ. If the number of open channels N is *not* equal to 0, the electric field (the slope of the potential curve) in this spatial region is approximately constant and homogeneous. The characteristic behavior of the imaginary part of the electric potential is shown in Figs. 2(b), 3(b), and 4(b). Note that both parts of the potential, $\phi'(\zeta)$ and $\phi''(\zeta)$, give a significant contribution to the admittance y.

For dimensionless frequency $\beta'=0$, corresponding to a dc applied field, the electric field in the region $|\zeta|<\zeta_{N+1}$ is small [see Figs. 2(a) and 3(a)]. For $\beta'\neq0$, the electric field [slope of $\phi'(\zeta)$] increases with increasing values of $\beta'=\mathrm{Re}\,\beta$ ($\sim$ frequency ω) *and* $\beta''=\mathrm{Im}\,\beta$ ($\sim$ relaxation rate ν). The imaginary part of the potential, $\phi''(\zeta)$, is a nonmonotonic function of β' [see Fig. 2(b)], and its slope increases monotonically with increasing β'' [see Fig. 3(b)]. Outside the interval $-\zeta_{N+1}<\zeta<\zeta_{N+1}$, the potential displays stepwise oscillations. The amplitude of these oscillations decreases as $|\zeta|$ increases [Figs. 2(b) and 3(b)]. We emphasize that the potential is a nonmonotonic function of the longitudinal coordinate ζ. In particular, there are intervals of ζ in which the direction of the local electric field is opposite to the direction of the external electric field applied to the contact.

When all channels are closed ($N=0$), the QPC behaves like a capacitor. In this case, the potential drop in the region between the first turning points, $|\zeta|<\zeta_1$, is of the order of the total voltage applied to the contact [see Fig. 6(a)], and the potential distribution in this region is significantly inhomogeneous. The imaginary part of the potential for this case is shown in Fig. 6(b).

Essentially new effects are observed when the value of q is close to the integer: $q\sim n_0\equiv N+1$, where N is the last open channel so that $N+1$ is the first closed channel. Figure 7 demonstrates the potential profiles for different values of β', and when q is slightly *below* an opening point [$q=1.96$ ($q<n_0=N+1=2$)]. The curves 1–6 in Figs. 7(a) and 7(b) correspond to the different values of the scaled applied frequency β'. From Figs. 7(a) and 7(b), one sees that both the real and imaginary parts of the potential have a frequency-dependent peak at the turning points, ζ_n. The physical location of the turning points is independent of frequency. The amplitude of these oscillations has a maximum when ζ is in the region $\zeta_{N+1}\leqslant|\zeta|\leqslant\zeta_{N+2}$. There are intervals of the frequency β' where the jumps of the real or

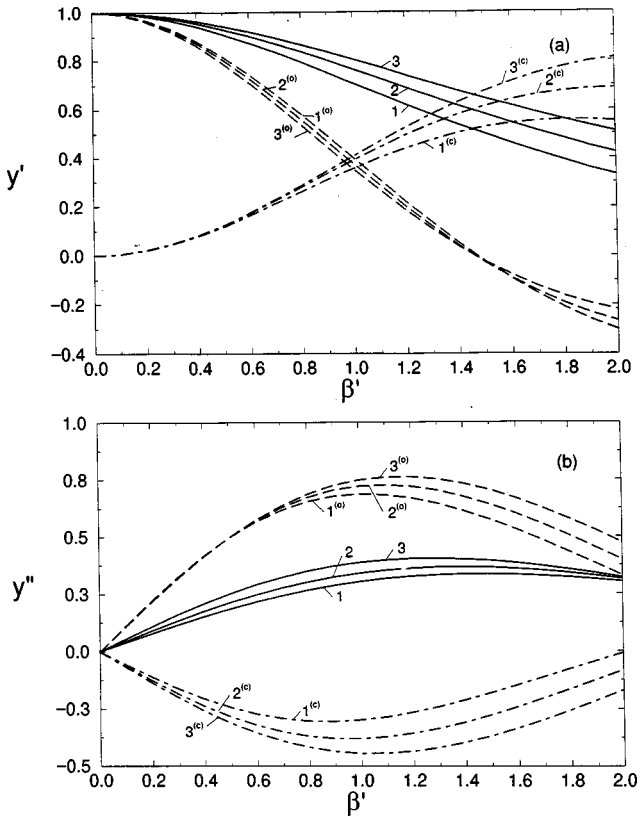

FIG. 5. Frequency dependence of (a) the real (y') and (b) the imaginary (y'') parts of the admittance y for $q=1.7$ ($N=1$), $\nu=0$, $\tilde{L}=10^{-3}$ cm and different values of L: (1) $L/\tilde{L}=1.0$, (2) $L/\tilde{L}=1.2$, (3) $L/\tilde{L}=1.4$. Also shown are the contributions to the admittance from the open (o) and the closed (c) channels.

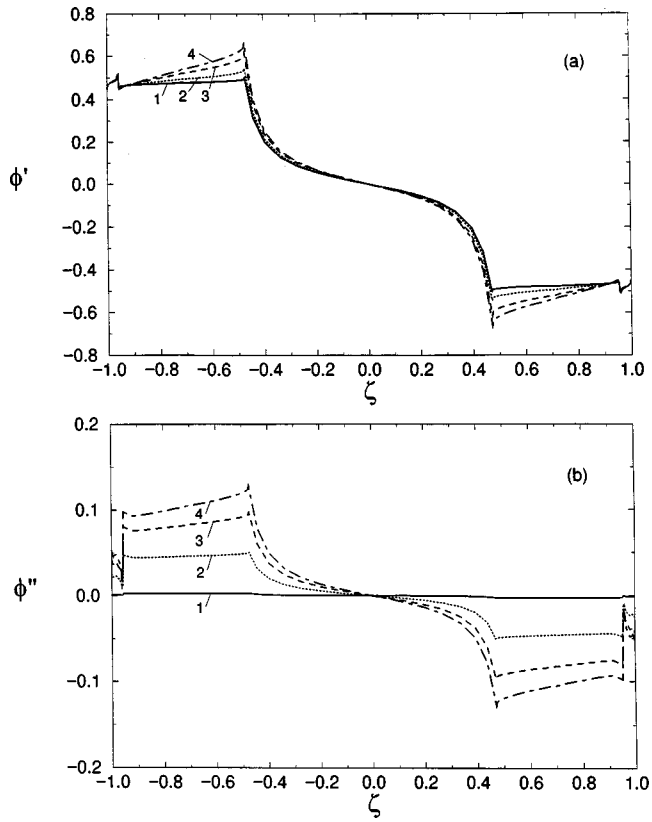

FIG. 6. The real part (a) and the imaginary part (b) of the potential distribution $\phi(\zeta)$ when the open channels are absent, $N=0$ [$d(0)=0.84\times10^{-6}$ cm, $L=\tilde{L}=10^{-3}$ cm, $q=0.8$, $\tilde{N}=2$] for $\nu=0$. The curves: (1) $\beta'=0.1$ ($\omega=2.6\times10^{9}$ s^{-1}), (2) $\beta'=1.6$ ($\omega=4.2\times10^{10}$ s^{-1}), (3) $\beta'=2.5$ ($\omega=6.5\times10^{10}$ s^{-1}), and (4) $\beta'=2.9$ ($\omega=7.5\times10^{10}$ s^{-1}).

imaginary parts of the potential at the point ζ_{N+1} (or $-\zeta_{N+1}$) are opposite in sign to the jumps at the points ζ_n (or $-\zeta_n$), $n=N+2,\ldots,N+\tilde{N}$. Moreover, there are values of β', at which the jumps of the real part of the potential at the point $|\zeta|=\zeta_{N+1}$ are significantly suppressed [see Fig. 7(a)]. For the imaginary part of the potential the jumps at the points $\pm\zeta_n$ can be suppressed by the proper choice of the frequency, and the jumps can change sign [see, e.g., curve 3 in Fig. 7(b)]. The oscillatory behavior of the real part of the potential as a function of *frequency* is shown in Fig. 8, with the different curves corresponding to different values of ζ within the QPC, as explained in the caption.

The situation when q is slightly *above* an opening point is illustrated in Fig. 9, where $q=2.01$ (so that the number of open channels is $N=2$). The dependence of the potential on β' has many features similar to the previous case of $q=1.96$ (Fig. 7), but the actual form of the potential is somewhat more complicated. Again, there are strong spatial oscillations of the potential in the region $-\zeta_{N+1}<\zeta<\zeta_{N+1}$. The curves 1–4 in Figs. 9(a) and 9(b) correspond to different values of frequency β'.

The solution of the integral equation (23) allows us to calculate the admittance $y=y'+iy''$, using Eqs. (28)–(30). Figures 10(a) and 10(b) demonstrate the frequency dependence of the admittance when q is not close to an integer. Figure 10 shows the case of one open channel ($N=1$), while in Fig. 11 the case two open channel ($N=2$) is shown. The contribution from open and closed channels is indicated by the symbols (o) and (c), respectively. The solid curves 1–3 in Figs. 10(a) and 11(a) indicate the frequency dependence of the real part of the admittance (y') at three different values of the parameter q, whereas the solid curves 1–3 in Figs. 10(b) and 9(b) reflect the behavior of the imaginary part of the admittance (y'') at the same three values of the parameter q.

As one can see from Figs. 10 and 11, the imaginary part of the admittance is approximately a linear function of the frequency in the region of scaled frequency $\beta'<\beta'_c\approx0.5$, which corresponds to $\omega_c\approx10$ GHz for the QPC parameters of Ref. 26. For $\beta'<\beta'_c$, the contributions to the imaginary part of the admittance from the open channels $y''^{(o)}$ and from the closed channels $y''^{(c)}$ are not only linear but have opposite signs: the contribution of the open channels is positive, corresponding to an inductive behavior, whereas the contribution of the closed channels is negative, corresponding to a capacitive behavior. Hence, as we have previously shown,[20] in this frequency region one can consider a QPC as an equivalent electrical circuit consisting of a resistance and capacitance in parallel and in series with an inductance.

For $\beta'>\beta'_c$ (corresponding to $\omega>10$ GHz), our numerical results show strong nonlinearities in the dependence of both y' and y''. In this frequency region, one cannot characterize the QPC as having an effective capacitance and inductance, at least not using a simple equivalent circuit with static conductance, inductance, and capacitance, as in Ref. 20.

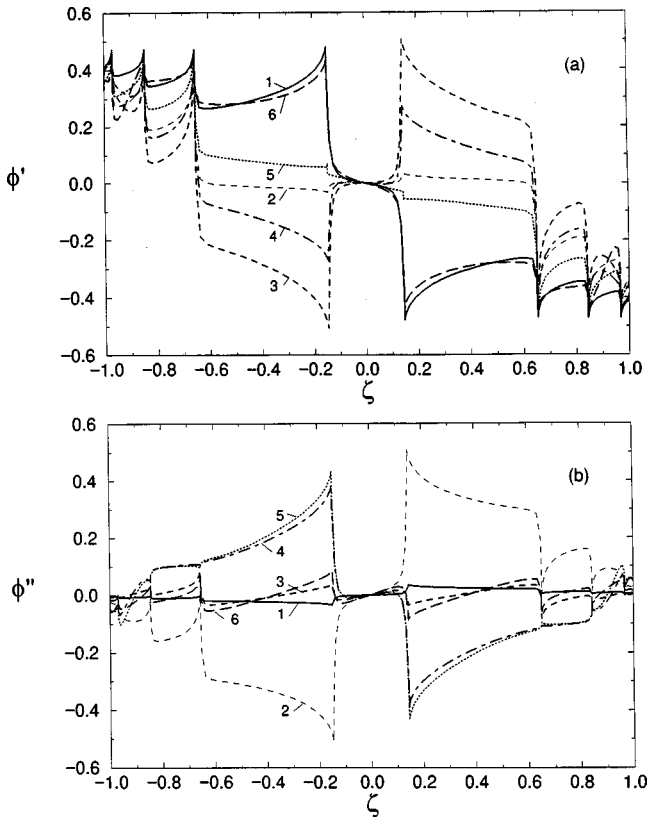

FIG. 7. The real (a) and the imaginary (b) parts of the potential distribution when the gate voltage is close to an opening point so that the value of q (here $q=1.96$) is close to an integer n_0 (here $n_0=2$), $q<n_0$. The opening point is the point where a new mode opens or closes. Curves 1–6 correspond to the following values of the frequency: (1) $\beta'=0.01$ ($\omega=2.6\times10^8$ s^{-1}), (2) $\beta'=0.23$ ($\omega=6.0\times10^9$ s^{-1}), (3) $\beta'=0.47$ ($\omega=1.2\times10^{10}$ s^{-1}), (4) $\beta'=0.60$ ($\omega=1.6\times10^{10}$ s^{-1}), (5) $\beta'=0.70$ ($\omega=1.8\times10^{10}$ s^{-1}), (6) $\beta'=0.85$ ($\omega=2.2\times10^{10}$ s^{-1}). The parameters of the QPC are $d(0)=2.05\times10^{-6}$ cm, $L=\tilde{L}=10^{-3}$ cm ($N=1,\tilde{N}=4$), $\nu=0$.

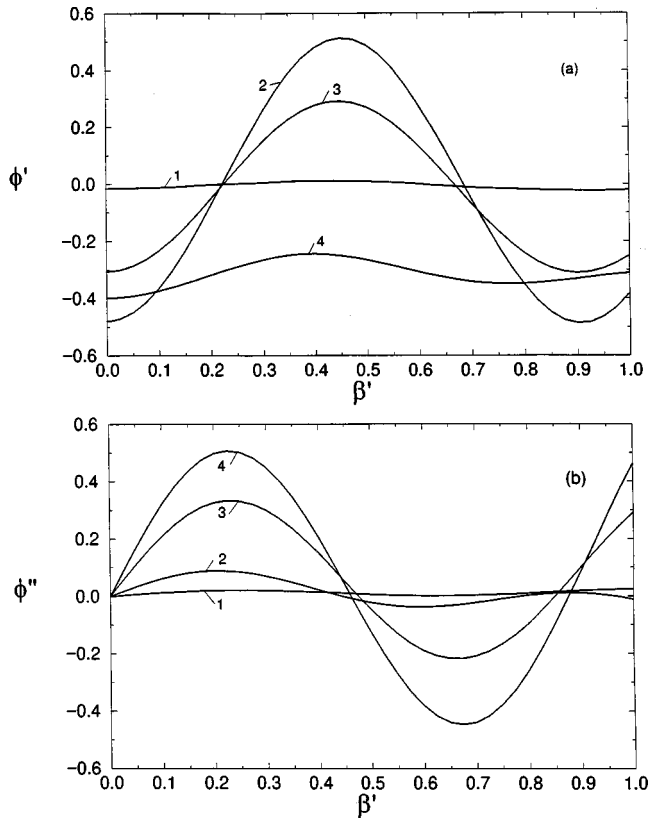

FIG. 8. The oscillating frequency dependence of (a) the real part and (b) the imaginary part of the potential for several specific values of ζ related to the turning points: (1) $\zeta=\zeta_{N+1}/2$, (2) $\zeta=\zeta_{N+1}$, (3) $\zeta=(\zeta_{N+1}+\zeta_{N+2})/2$, (4) $\zeta=(\zeta_{N+\tilde{N}-1}+\zeta_{N+\tilde{N}})/2$, where ζ_n ($n=N+1,\ldots,N+\tilde{N}$) is the coordinate of the turning point for the nth closed channel. As in Fig. 7, the parameters of the QPC are $d(0)=2.05\times10^{-6}$ cm, $L=\tilde{L}=10^{-3}$ cm ($N=1,\tilde{N}=4$), $\nu=0$.

Note that even in the frequency range where the linear approximation for $y''(\beta')$ applies well, the nonlinearity of the frequency dependence of $y'(\beta')$ is not negligible. Indeed, near $\beta'=0$, the curve $y'(\beta')$ as well as the curves $y'^{(o)}(\beta')$ and $y'^{(c)}(\beta')$ are approximately quadratic in most cases. [See Figs 10(a) and 11(a).] Note that the contribution of the nonpropagating modes $y'^{(c)}$ increases with increasing β', and the amount of the nonlinearity of $y'^{(c)}(\beta')$ increases when q approaches $N+1$. Note also that the nonlinear parts of the contributions of the open and closed channels have *opposite* signs. Thus, it is possible to choose a value of q such that the nonlinearities of $y'^{(o)}(\beta')$ and $y'^{(c)}(\beta')$ approximately compensate one another. In this case, the approximation $y'(\beta')\simeq\text{const}=y'(0)$ (the approximation of static conductance) can be used in a wide frequency range [curve 3 in Fig. 11(a)]. For the imaginary part of y, the nonlinear components of $y''^{(o)}$ and $y''^{(c)}$ depend on q in a more complicated manner. However, the value of q can be chosen such that the nonlinearities of these two contributions are partially compensated, and the approximation of the effective inductance and capacitance is valid for a wide range of β'.

We have already shown that there are strong oscillatory effects in $\phi(\xi)$ for q close to values at which channels open ($n_0=N+1$) or close ($n_0=N$). It is thus not surprising that we also find that the admittance oscillates as a function of the frequency (see Figs. 12 and 13) near these values of q. Indeed, as q approaches n_0, the frequency of these oscillations (in the case $\nu=0$) increases without bound, and the range of β' where the linear approximation for $y(\beta')$ is valid becomes smaller. Figures 12 and 13 show that the oscillating part of $y(\beta')$ is given by the contribution to the admittance from the n_0th channel [see curve 4 in Fig. 12(a)], i.e., by y_{n_0}. Note that although the number of open channels in Fig. 12 is only $N=1$, nonetheless the conductance increases to $y'(0.5)\approx2$. At this value of the frequency, effectively two open channels give a contribution to the conductance. Figure 12(b) shows that if $n_0=N+1$, then in the low-frequency region, the *closed* channels can give a positive (inductive[20]) contribution to $y''(\beta')$. This is in contrast to the case when q is not close to N or $N+1$, for which the closed channels at low frequencies are described by an effective capacitance [see Figs. 10(b) and 11(b)]. This surprising inductive contribution of the closed channels originates from the specific form of the potential distribution (see Fig. 7), in particular, from the fact that there are large spatial regions in the QPC in which the local electric field is opposed to the applied field.

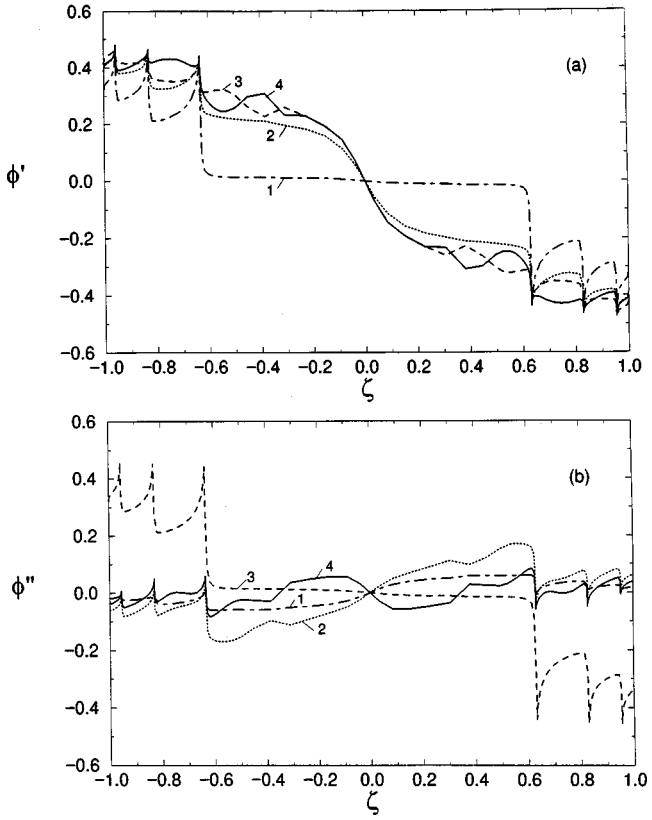

FIG. 9. The real (a) and the imaginary (b) parts of the potential distribution when q ($q=2.01$) is close to the integer $n_0=2$, but $q>n_0$. Curves 1–4 correspond to the following values of the frequency: (1) $\beta'=0.1$ ($\omega=2.6\times10^9$ s^{-1}), (2) $\beta'=0.7$ ($\omega=1.8\times10^{10}$ s^{-1}), (3) $\beta'=1.2$ ($\omega=3.1\times10^{10}$ s^{-1}), and (4) $\beta'=1.7$ ($\omega=4.4\times10^{10}$ s^{-1}). The parameters of the QPC are $d(0)=2.1\times10^{-6}$ cm, $L=\tilde{L}=10^{-3}$ cm ($N=2, \tilde{N}=3$), and $\nu=0$.

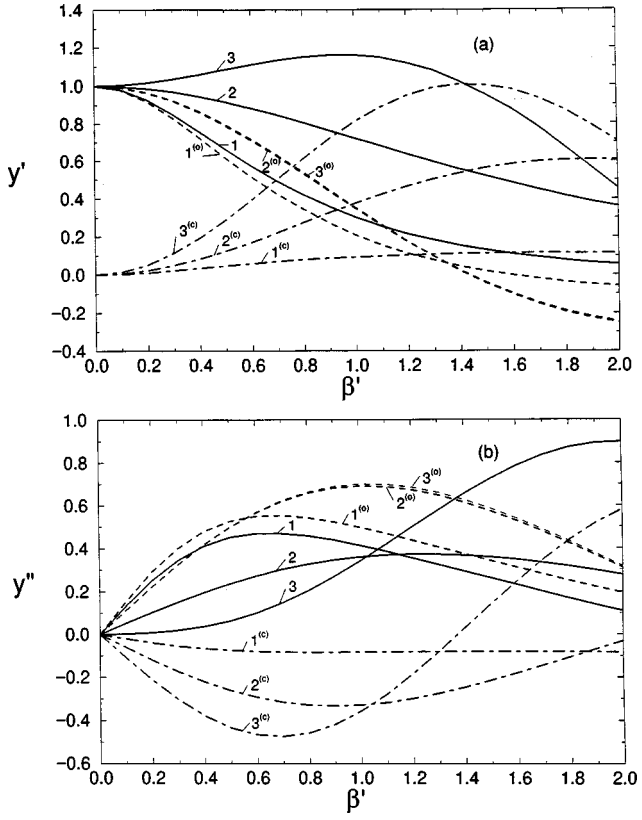

FIG. 10. Frequency dependence of the real (a) y' and the imaginary (b) y'' parts of the admittance y for different values of $q=2k_Fd(0)/\pi$, when $N=1$: (1) $q=1.1$ ($\tilde{N}=2$), (2) $q=1.7$ ($\tilde{N}=3$), (3) $q=1.75$ ($\tilde{N}=3$). The values of q are not close to the integer numbers N and $N+1$. Also shown are the contributions to the admittance from the open (o) and the closed (c) channels. The parameters are $L=10^{-3}$ cm and $\nu=0$, as in Figs. 6–9.

As a function of the parameter $q=2k_Fd(0)/\pi$ (or the gate voltage), the admittance exhibits stepwise variations that have been examined previously at low frequency.[17,18,20] We have obtained the specific form of these oscillations for several values of frequency. The dependence of the admittance on q for the case of low frequency is shown in Fig. 14. The real part of the low-frequency admittance [Fig. 14(a)] is determined by the number of propagating modes. Considering the imaginary part of the admittance [Fig. 14(b)], the contribution of the open channels is positive (inductive), and increases as the number of open channels increases. [Compare the curves $y_1''^{(o)}$ and $y_2''^{(o)}$ in Fig. 14(b).] The contribution of the closed channels, $y^{(c)}$, depends on q in a more complicated manner. For q not close to $N+1$ this contribution is negative (capacitive, see curve $y_{1,2}''^{(c)}$), but when q approaches $N+1$, $y_{1,2}''^{(c)}$ increases and becomes positive (inductive). As mentioned above, the inductive character of $y''^{(c)}(\beta')$ for q near $N+1$ can be explained by the peculiarities of the potential distribution inside the QPC. The imaginary part of the total admittance, $y''=y''^{(o)}+y''^{(c)}$, can have a capacitive character only for $N=0,1$. For larger N, the total imaginary part y'' is positive (inductive) because the contribution of the open channels dominates. For sufficiently high frequencies, we found oscillating behavior of $y(q)$ for q in the vicinities of integers (Fig. 15). These oscillations are connected with the fact that for fixed value of frequency ω, the characteristic residence time $\tau_n(x,x')$ in Eq. (3) increases logarithmically as an electron approaches a separatrix [$\mu=\varepsilon_n(0)$, or $q=n$]. In this case, a small variation of q leads to a large variation of the phase in Eqs. (4) and (5).

IV. CONCLUSIONS

In the present paper, we have numerically studied the spatial distribution of the potential, $\phi(\zeta)$ and the resulting frequency dependence of the admittance $y(\omega)$ in a QPC. We employed a semiclassical, single-particle approximation, assuming ballistic electron transport and treating the effects of the Coulomb interaction in a self-consistent manner (i.e., we neglected many-body direct Coulomb interactions). Using the results of transport theory based on the partial Wigner distribution function formalism,[20] in combination with the Poisson equation, we derived an integral equation for the spatial distribution of the electric field in the QPC. We solved this equation numerically for different values of QPC parameters and for a wide range of frequencies, $\omega\approx0-50$ GHz. We found that the electric potential inside the QPC is a stepwise function of the dimensionless longitudinal coordinate ζ with peaks in the potential profile located at the turning points $\pm\zeta_n$ of the semiclassical motion. The poten-

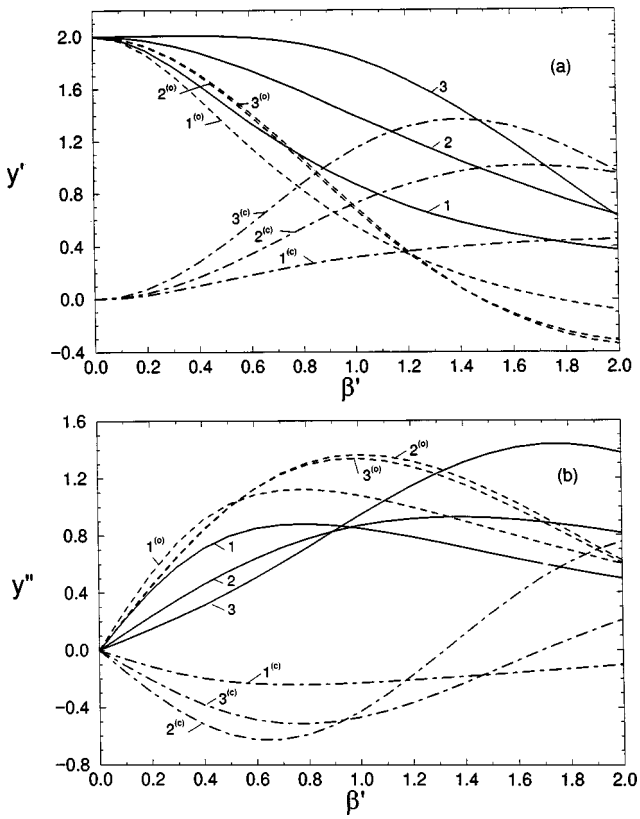

FIG. 11. Frequency dependence of the admittance for different values of q, for $N=2$: (1) $q=2.1$ ($\tilde{N}=3$), (2) $q=2.7$ ($\tilde{N}=5$), (3) $q=2.8$ ($\tilde{N}=5$), and for the same parameters $L,\tilde{L},\nu$ as in Fig. 10. Also shown are the contributions to the admittance from the open (o) and the closed (c) channels.

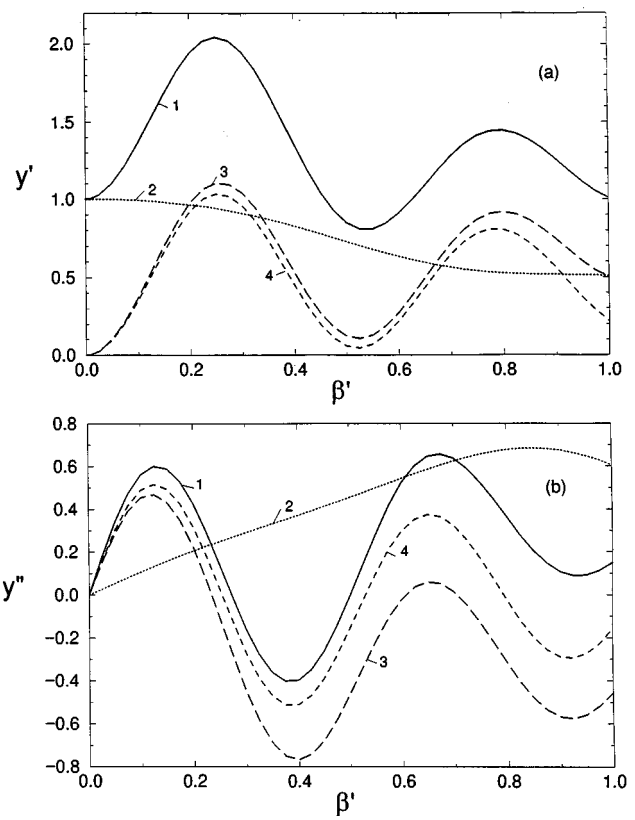

FIG. 12. Frequency dependence of the real (a) and the imaginary (b) parts of the admittance, when q ($q=1.96$) is close to an integer n_0 ($n_0=N+1=2$), $q<n_0$. The contributions to y (curves 1) from the open channels (curves 2), the closed channels (curves 3), and from the $(N+1)$th closed channel (curves 4) are shown. As in Fig. 7, the values of the parameters are $d(0)=2.05\times10^{-6}$ cm, $L=\tilde{L}=10^{-3}$ cm ($N=1,\tilde{N}=4$), $\nu=0$.

tial is not a monotonic function of ζ, and indeed there are spatial regions in which the local electric field is opposite to the direction of the applied external field.

We studied the dependence of the potential profile on the frequency of the applied electric field. When the gate voltage is near a value at which a channel opens or closes, and if the frequency is sufficiently high, the form of the potential profile differs significantly from the potential profile in the static case. Moreover, the value of the potential for a fixed spatial point ζ oscillates as a function of frequency.

We considered the dependence of the admittance on the frequency ω and on the gate voltage [or the parameter $q=2k_Fd(0)/\pi$]. Near $\omega=0$, a linear approximation for the frequency dependence of the admittance is valid. In this low-frequency regime, one can use the approximation of static conductance for the real part of the admittance and the approximation of an effective inductance and capacitance for the imaginary part to obtain an equivalent electric circuit model of the QPC.[20] The size of this low-frequency regime depends on the gate voltage, and we have shown that one can choose the value of the gate voltage so that the linear approximation for the admittance is valid for a wide range of frequencies, up to $\omega\sim10$ GHz for chosen QPC parameters. Physically, the reason for the validity of the linear approximation over a wide range is that the *nonlinear* components of the contributions to the admittance from the open and closed channels have opposite signs and can thus compensate each other.

Nonlinear effects are substantially enhanced when the gate voltage is close to one of the opening points [the value of $2k_Fd(0)/\pi$ is close to an integer n_0]. Here both the real and imaginary parts of the admittance oscillate as the functions of frequency. The period of these oscillations decreases when the gate voltage approaches an opening point. The oscillations are mainly determined by the n_0th electron channel, which can be understood as follows. The oscillations are significant when the characteristic time of the effective electron motion along the one-dimensional trajectory (see Ref. 20) is of the order of the period of the electric field. If $2k_Fd(0)/\pi$ is close to n_0, the time of the electron motion in the QPC is much larger for the n_0th channel than for the other channels. Thus, for the n_0th electron channel strong frequency dependence can be realized at much lower frequencies.

As a function of the gate voltage, the admittance has stepwise oscillations (see Refs. 17, 18, and 20). We obtained the specific form of these steps. For the case of low frequencies, the contribution of the open channels is positive (inductive). When q is not close to the integer, $N+1$, the contribution of the closed channels is negative (capacitive). However, as q approaches $N+1$, the contribution from the closed channels

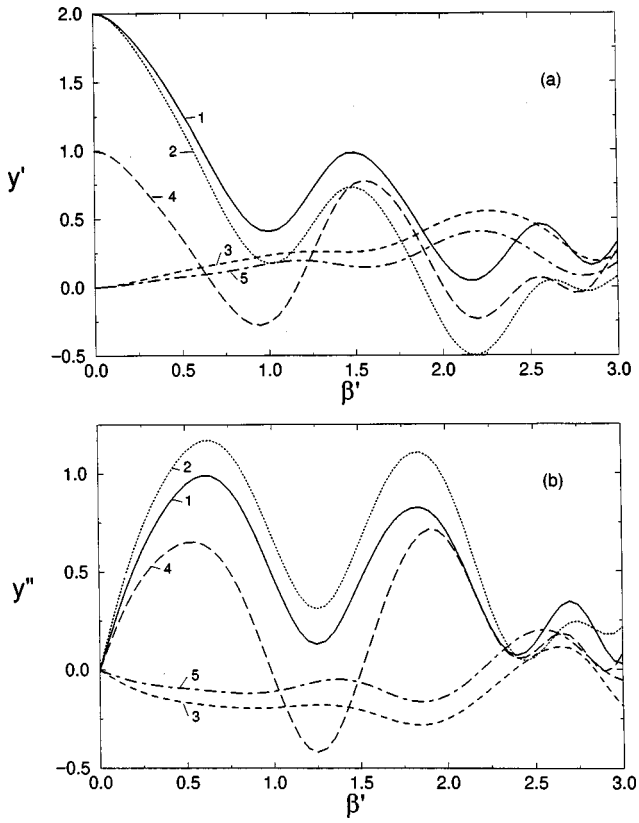

FIG. 13. Oscillations of the frequency dependence of the real (a) and the imaginary (b) parts of the admittance y (curves 1) when $q=2.005\,(q>n_0,\, n_0=N=2)$. The contributions from the open channels (curves 2), the closed channels (curves 3), the Nth open channel (curves 4), and the $N+1$st closed channel (curves 5) are shown. As in Fig. 9, the parameters of the QPC are $d(0)=2.1\times10^{-6}$ cm, $L=\tilde{L}=10^{-3}$ cm $(N=2, \tilde{N}=3)$, and $\nu=0$.

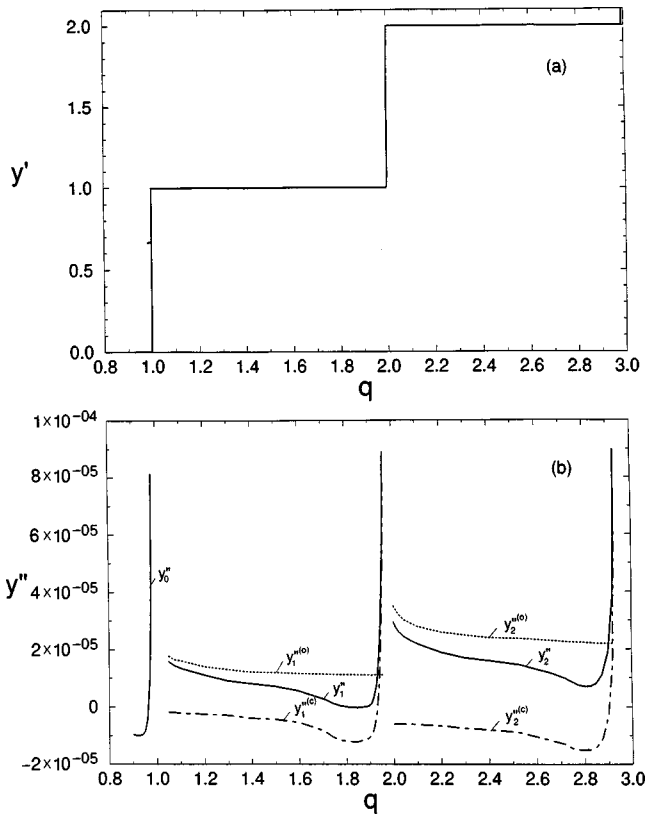

FIG. 14. Dependence of the real (a) and the imaginary (b) parts of the low-frequency admittance y $(\beta'=10^{-5},\ \omega=2.6\times10^{5}\ \mathrm{s}^{-1})$ on the value of q (the gate voltage). In (b) the contributions of the open (curves 2) and closed (curves 3) channels are shown. The parameters are $L=\tilde{L}=10^{-3}$ cm and $\nu=0$.

becomes positive (inductive). This behavior is caused by the existence within the QPC of large spatial regions in which the local electric field is opposite to the applied field (see Fig. 7). For $N>1$, the frequency dependence of the imaginary part of the total admittance has an inductive character because of the predominant role of the open channels. If $N=0$ or 1, we have found that overall capacitive behavior of the QPC is possible. In this connection, it is important to compare our results with a previous study of the low-frequency admittance of a QPC.[17] We shall focus primarily on the final results of Ref. 17 for the emittance, which are shown in (the full curve in) Fig. 2 of Ref. 17 (see p. 146). To compare the two sets of results, one must recall that in Fig. 2 of Ref. 17 the authors plot the *emittance* E, while in Fig. 14(b) of our paper, we plot the imaginary part of the *admittance*: the relation is $y''=-\omega E$, so E and y'' have different signs. In Fig. 2 of Ref. 17, for the barrier height eU_0 (roughly, corresponding to our gate voltage) varying from zero (allowing three open channels) to approximately 7 meV (allowing no open channels), the emittance is negative, i.e., the imaginary part of the admittance is positive, and, in our terminology, the behavior of the QPC is inductive. So, for the number of open channels $N=3,2,1$ the admittance is inductive. (In Fig. 2 of Ref. 17 the number of open channels N is indicated by the conductance curve plotted as the dashed line.) Only when the value of eU_0 approaches the opening point at which the last open channel closes $(N\to0)$ does the emittance curve become positive (capacitive). Hence, only for $N=0$ is the total admittance capacitive in Fig. 2 in Ref. 17. Our more detailed calculations agree in general with these results, showing effective inductive (positive, in our convention) behavior for $N>1$. However, our self-consistent solution leads to a spatially inhomogeneous electric field, which in turn generates a more complicated structure of peaks in the total admittance curve than would follow from the approach of Ref. 17. One consequence is that we find a small region—near $q=1.8$ for the other parameters we have chosen (so that $N=1$)—in which the admittance is capacitive (negative, in our convention). For $N=0$, of course, we also have capacitive behavior, as found previously.[17]

In view of the importance of understanding the ac transport through QPC's and related nanostructures—both for developing the appropriate physical picture and for suggesting or optimizing novel devices for applications—there are many additional studies that we plan to undertake, among them further investigations to determine the responses of specific experimental QPC configurations and to understand the limits of validity of the semiclassical approach adopted here. We are also hopeful that additional experimental studies of the ac admittance of QPC's will observe the oscillations both as a function of gate voltage (at fixed frequency) and as a function of frequency (at fixed gate voltage) predicted by our semiclassical theoretical considerations.

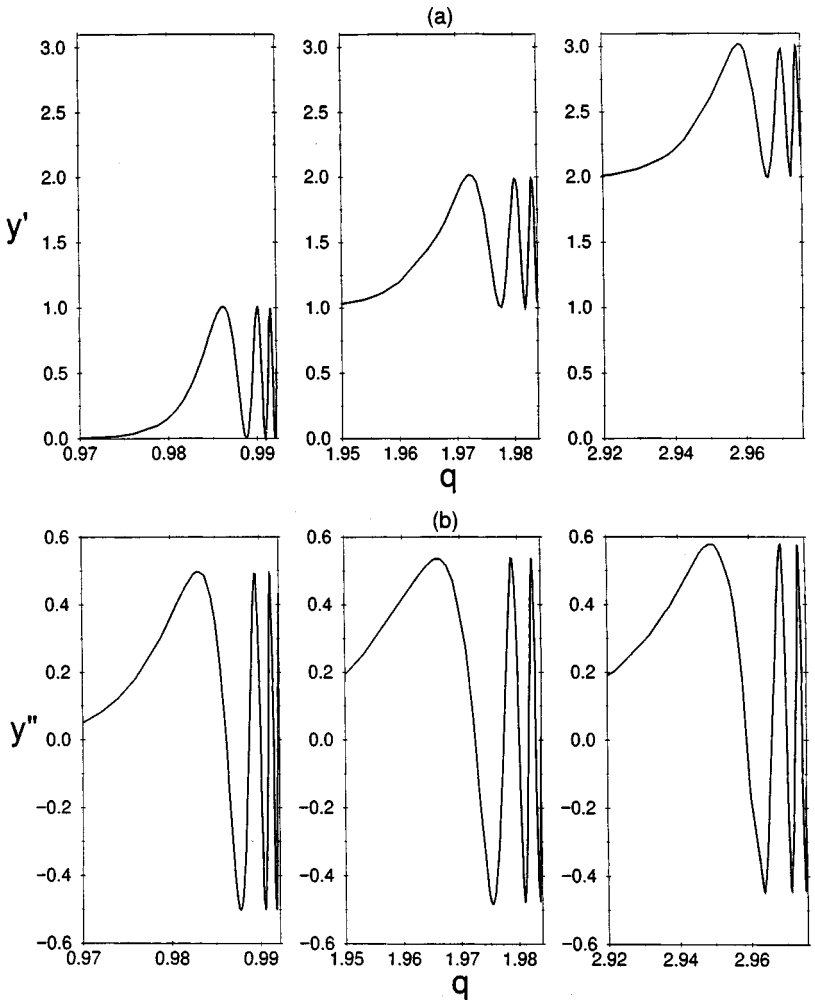

FIG. 15. The oscillating dependence of (a) the real and (b) the imaginary parts of the admittance y on q, when q is in the vicinity of the integer (for $\beta' = 0.05$, $\omega = 1.3 \times 10^9$ s^{-1}).

ACKNOWLEDGMENTS

We are grateful to L. I. Glazman, D. K. Ferry, and E. H. Cannon for fruitful discussions and suggestions. This research was supported in part by the Linkage Grant No. 93-1602 from the NATO Special Programme Panel on Nanotechnology, by Grant No. 94-02-04410 of the Russian Fund for Basic Research, by INTAS Grant No. 94-3862, and by the Ukrainian Committee for Science and Technology (Project No. 2.3/19 ''Metal''). The work at LANL was supported by the Defense Advanced Research Projects Agency.

[1] L. I. Glazman, G. B. Lesovik, D. E. Khmelnitskii, and R. I. Shekhter, JETP Lett. **48**, 238 (1988).

[2] C. W. J. Beenakker and H. van Hasten, in *Solid State Physics*, edited by H. Ehrenreich and D. Turnbull (Academic, San Diego, 1991), Vol. 44, p. 1.

[3] B. J. van Wees, H. van Houten, C. W. J. Beenakker, J. G. Williamson, L. P. Kouwenhoven, D. van der Marel, and C. T. Foxon, Phys. Rev. Lett. **60**, 848 (1988).

[4] D. A. Wharam, T. J. Thornton, R. Newbury, M. Pepper, H. Ahmed, J. E. F. Frost, D. G. Hasko, D. C. Peacock, D. A. Ritchie, and G. A. C. Jones, J. Phys. C **21**, L209 (1988).

[5] B. J. van Wees, L. P. Kouwenhoven, H. van Houten, C. W. J. Beenakker, J. E. Mooij, C. T. Foxon, and J. J. Harris, Phys. Rev. B **38**, 3625 (1988).

[6] N. K. Patel, J. T. Nicholls, L. Martin-Moreno, M. Pepper, J. E. F. Frost, D. A. Ritchie, and G. A. C. Jones, Phys. Rev. B **44**, 13 549 (1991).

[7] R. Taboryski, A. K. Geim, and P. E. Lindelof, Superlattices Microstruct. **12**, 137 (1992); R. Taboryski, A. K. Geim, M. Persson, and P. E. Lindelof, Phys. Rev. B **49**, 7813 (1994).

[8] T. M. Eiles, J. A. Simmons, M. E. Sherwin, and J. F. Klem, Phys. Rev. B **52**, 10 756 (1995).

[9] L. I. Glazman and M. Jonson, Phys. Rev. B **41**, 10 686 (1990).

[10] I. E. Aronov, M. Jonson, and A. M. Zagoskin, Phys. Rev. B **50**, 4590 (1994).

[11] A. Grincwajg, M. Jonson, and R. I. Shekhter, Phys. Rev. B **49**, 7557 (1994); L. Y. Gorelik, A. Grincwajg, V. Z. Kleiner, R. I. Shekhter, and M. Jonson, Phys. Rev. Lett. **73**, 2260 (1994); A. Grincwajg, L. Y. Gorelik, V. Kleiner, and R. I. Shekhter, Phys. Rev. B **52**, 12 168 (1995).

[12] F. Hekking and Yu. V. Nazarov, Phys. Rev. B **44**, 11 506 (1991); **44**, 9110 (1991).
[13] M. Büttiker, H. Thomas, and A. Prêtre, Phys. Lett. A **180**, 364 (1993).
[14] M. Büttiker, J. Phys.: Condens. Matter **5**, 9361 (1993).
[15] M. Büttiker, Nuovo Cimento B **110**, (5-6), 509 (1995).
[16] M. Büttiker, in *Quantum Dynamics of Submicron Structures*, edited by H. A. Cerdeira *et al.* (Kluwer-Academic, The Netherlands, 1995), pp. 657–672; W. Chen, T. P. Smith III, M. Büttiker, and M. S. Shayegan, Phys. Rev. Lett. **73**, 146 (1994).
[17] T. Christen and M. Büttiker, Phys. Rev. Lett. **77**, 143 (1996).
[18] T. Christen and M. Büttiker, Phys. Rev. B **53**, 2064 (1996).
[19] A. Prêtre, H. Thomas, and M. Büttiker, Phys. Rev. B **54**, 8130 (1996).
[20] I. E. Aronov, G. P. Berman, D. K. Campbell, and S. V. Dudiy, J. Phys.: Condens. Matter **9**, 5089 (1997).
[21] H. M. Pastawski, Phys. Rev. B **44**, 6329 (1991); **46**, 4053 (1992).
[22] J. Wang, Q. R. Zheng, and H. Guo, Phys. Rev. B **55**, 9770 (1997).
[23] Y. Fu and S. C. Dudley, Phys. Rev. Lett. **70**, 65 (1993); C. Jacoboni and J. P. Price, *ibid.* **71**, 464 (1993); Y. Fu and S. C. Dudley, *ibid.* **71**, 466 (1993).
[24] A. L. Fetter, Ann. Phys. (N.Y.) **81**, 367 (1973).
[25] I. S. Gradshteyn and I. M. Ryzhik, *Table of Integrals, Series, and Products* (Academic, New York, 1965).
[26] D. Mailly, C. Chapelier, and A. Benoit, Phys. Rev. Lett. **70**, 2020 (1993).
[27] W. H. Press, S. A. Teukolsky, W. T. Vetterling, and B. P. Flannery, *Numerical Recipes in C* (Cambridge University Press, New York, 1992).
[28] L. M. Devles and J. L. Mohamed, *Computational Methods for Integral Equations* (Cambridge University Press, New York, 1985).